Crystallization and preliminary X-ray diffraction studies of FHA domains of Dun1 and Rad53 protein kinases

Helen Blanchard,[a,b]*[†]
Marcos R. M. Fontes,[b][†][‡] Andrew Hammet,[b][†] Brietta L. Pike,[b][†]
Trazel Teh,[b] Thomas Gleichmann,[b] Paul R. Gooley,[c] Bostjan Kobe[a,b] and Jörg Heierhorst[b]

[a]Department of Biochemistry, University of Queensland, St Lucia, Brisbane, Qld 4072, Australia, [b]St Vincent's Institute of Medical Research, 41 Victoria Parade, Fitzroy, Vic 3065, Australia, and [c]Department of Biochemistry and Molecular Biology, University of Melbourne, Parkville, Vic 3052, Australia

† These authors contributed equally to this work.
‡ On leave from Departamento de Física e Biofísica, Instituto de Biociências, UNESP, Botucatu-SP, Brazil.

Correspondence e-mail: helenb@biosci.uq.edu.au

Forkhead-associated (FHA) domains are modular protein–protein interaction domains of ~130 amino acids present in numerous signalling proteins. FHA-domain-dependent protein interactions are regulated by phosphorylation of target proteins and FHA domains may be multifunctional phosphopeptide-recognition modules. FHA domains of the budding yeast cell-cycle checkpoint protein kinases Dun1p and Rad53p have been crystallized. Crystals of the Dun1-FHA domain exhibit the symmetry of the space group $P6_122$ or $P6_522$, with unit-cell parameters $a = b = 127.3$, $c = 386.3$ Å; diffraction data have been collected to 3.1 Å resolution on a synchrotron source. Crystals of the N-terminal FHA domain (FHA1) of Rad53p diffract to 4.0 Å resolution on a laboratory X-ray source and have Laue-group symmetry 4/mmm, with unit-cell parameters $a = b = 61.7$, $c = 104.3$ Å.

1. Introduction

Many signalling molecules contain non-catalytic modules as part of their polypeptide chains and these modules play crucial roles in accomplishing the assembly of signalling complexes (Pawson & Scott, 1997). The forkhead-associated (FHA) domains are one class of protein-interaction modules present in a diverse set of over 120 signalling proteins, covering all phyla from bacteria, yeast and plants to mammals (Hofmann & Bucher, 1995). In human cells, FHA domains seem to be particularly prevalent in so-called checkpoint proteins that delay the cell cycle in response to replicational stress and DNA damage (*e.g.* Chk2, Nbs1) or mitotic spindle-assembly defects (*e.g.* CHFR; Scolnick & Halazonetis, 2000). This way, FHA domain-containing proteins act as tumour-suppressor molecules and their mutation leads to a genetic predisposition to cancer. For example, the FHA-domain-containing protein kinase Chk2 is mutated in a subset of patients suffering from the Li–Fraumeni multicancer syndrome (usually caused by mutations in p53; Bell *et al.*, 1999) and disease-causing mutations in the FHA-domain-containing protein Nbs1 are documented in a large subset of patients with Nijmegen breakage syndrome (Carney *et al.*, 1998). The importance of FHA-domain-containing checkpoint proteins is further illustrated by the fact that they, as well as the respective signalling pathways, are highly conserved throughout evolution from the yeasts *Saccharomyces cerevisiae* and *S. pombe*

to humans (Elledge, 1996; Rhind & Russel, 1998).

Dun1p and Rad53p are budding yeast homologues of the human Chk2 kinase. While Dun1p has a similar topology to Chk2 with a single FHA domain located N-terminal to the kinase catalytic domain, Rad53p contains FHA domains both N-terminal (FHA1) as well as C-terminal (FHA2) to the kinase domain. The FHA2 domain is essential for the DNA damage-induced activation of Rad53p by mediating its interaction with phosphorylated Rad9p *in vivo* (Sun *et al.*, 1998). The *in vivo* function of the FHA1 domain is unknown, but recent evidence indicates that it can directly bind to phosphothreonine-containing peptides *in vitro* (Durocher *et al.*, 1999). Based on overexpression experiments, the Dun1-FHA domain appears to be involved in the Dun1-dependent transcriptional induction of repair enzymes in response to replication blocks *in vivo* (Hammet *et al.*, 2000). The recent NMR structure of the Rad53-FHA2 domain has provided the first insight into the overall structure of FHA domains (Liao *et al.*, 1999). The core of the FHA2 domain is formed by an 11-stranded β-sandwich similar to the MH2 domain of smad transcription factors. The FHA2 domain also interacts with phospho-tyrosine, indicating that FHA domains may be multifunctional phosphopeptide-binding modules. The NMR structure as well as recent biochemical studies (Hammet *et al.*, 2000) have demonstrated that FHA domains in yeast checkpoint kinases contain >130 amino-acid residues and are therefore considerably larger

than the 55–75 amino-acid segment predicted by sequence comparisons. However, based on limited proteolysis experiments the Dun1-FHA and Rad53-FHA1 domains seem to contain some 20 residues at the N-terminus that are missing from the stable Rad53-FHA2 fragment (573–730) used for the NMR structure. To further our understanding of FHA domain structures and ultimately of the mechanism of phosphopeptide recognition by these modules, we have initiated structural studies of the Dun1-FHA and Rad53-FHA1 domains, both containing extended N-terminal regions compared with the FHA2 fragment in the NMR structure. This report describes the preliminary crystallographic characterization of these domains.

2. Materials and methods

2.1. Protein expression and purification

Constructs corresponding to proteolytically stable FHA domains (residues 19–159 of Dun1p; residues 20–164 of Rad53p) were generated by the polymerase chain reaction. These fragments were cloned into pQE60 and expressed and purified essentially as described previously for larger fragments (Hammet et al., 2000).

2.2. Crystallization

Crystallization conditions were screened by the sparse-matrix approach and an ammonium sulfate grid screen using the hanging-drop vapour-diffusion technique (Jancarik & Kim, 1991; McPherson, 1982) at 277 and 293 K. After 1 d, very small crystals ($\sim$0.01 $\times$ 0.02 $\times$ 0.02 mm) of Dun1-FHA grew when combining an equal ratio of protein solution (11.5–14 mg ml^{-1} in 20 mM imidazole at pH 7.0) and reservoir solution consisting of 2.4 M (NH$_4$)$_2$SO$_4$ and suspending over 1.0 ml of the reservoir solution at 293 K. The crystals have a hexagonal morphology (Fig. 1) and repeated

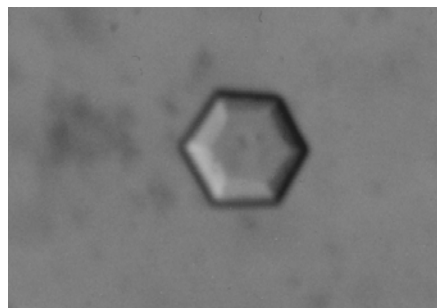macroseeding was required to increase the crystal size to 0.1 $\times$ 0.2 $\times$ 0.2 mm. Crystals of Rad53-FHA1 were obtained after 2 d when combining an equal ratio of protein solution (15 mg ml^{-1}) and reservoir solution consisting of 0.1 M HEPES pH 7.5, 10%(v/v) 2-propanol and 20%(w/v) polyethylene glycol 4000 at 293 K. However, these crystals were of poor morphology and diffraction quality. Modification of these conditions to 0.1 M HEPES pH 7.0, 10%(v/v) 2-propanol or ethanol, 18%(w/v) polyethylene glycol 4000 and 277 K yielded a few crystals suitable for X-ray crystallographic studies after two months.

2.3. X-ray data collection and processing

A crystal of Dun1-FHA with dimensions of 0.1 $\times$ 0.2 $\times$ 0.2 mm was transiently soaked in cryoprotectant solution containing 30% glycerol and 2.4 M (NH$_4$)$_2$SO$_4$. The crystal was flash-cooled at 100 K in a nitrogen stream (Oxford Cryosystems Cryostream) and X-ray diffraction data were collected at Stanford Synchrotron Radiation Laboratory (SSRL) beamline 9-1 (λ = 0.97 Å) using a MAR Research 345 image-plate detector. The data-collection strategy incorporated oscillation angles of 0.25, 0.5 and 1° in order to accommodate regional variations in overlapping reflections and exposure times of 45–180 s. Data were processed at 3.1 Å resolution and scaled using the programs DENZO and SCALEPACK (Otwinowski & Minor, 1997); the statistics are given in Table 1.

A crystal of Rad53-FHA1 with dimensions of 0.2 $\times$ 0.1 $\times$ 0.05 mm was mounted in a quartz capillary and X-ray diffraction data were collected at 290 K using Cu $K\alpha$ radiation from a Rigaku RU-200 X-ray generator operating at 90 mA and 50 kV with a MAR Research 345 imaging-plate detector. Initially the crystals diffracted to 3 Å resolution, but the high-resolution diffraction rapidly weakened during the data collection owing to radiation damage. Data were processed and scaled at 4.0 Å resolution (Table 1) using the programs DENZO and SCALEPACK (Otwinowski & Minor, 1997).

3. Results and discussion

The Dun1p FHA data set (Table 1) is 98.2% complete at 3.1 Å and is reasonably complete (>95%) throughout all resolution shells, with 72% of data

having $I > 3\sigma(I)$. The crystals exhibit a hexagonal lattice, with unit-cell parameters $a = b = 127.3$, $c = 386.3$ Å. The Laue symmetry of 6/mmm was indicated clearly from scaling statistics; systematic absences along the sixfold axis enabled distinction between $P6_122$/$P6_522$ ($l = 6n$) and $P6_222$/$P6_422$ ($l = 3n$). Assuming 12 molecules of Dun1-FHA (the molecular mass of Dun1-FHA is 17 233 Da) per asymmetric unit, the V_M (Matthews, 1968) is 2.2 Å^3 Da^{-1}, corresponding to a crystal solvent content of 44%. Molecular-replacement calculations (Collaborative Computational Project, Number 4, 1994; MOLREP; Vagin & Teplyakov, 1997) are being attempted using a homology model derived from the NMR structure of Rad53-FHA2 (Liao et al., 1999). Simultaneously, we are attempting to prepare heavy-atom derivative crystals and also a selenomethionine-labelled derivative of Dun1-FHA, which contains one methionine. We aim to determine these structures using the techniques of multiple isomorphous replacement (MIR), molecular replacement (MR) and multi-wavelength anomalous dispersion (MAD).

The Rad53-FHA1 data set (Table 1) is 93.3% complete at 4.0 Å; however, the data are weak [45% of data with $I > 3\sigma(I)$] and merge poorly (R_{merge} = 33.0%) as a consequence of the radiation damage to the crystal. The crystals have a tetragonal lattice, with unit-cell parameters $a = b = 61.7$, $c = 104.3$ Å. Owing to the insufficient data information on systematic absences it is not possible to determine the space group at this stage. However, the Laue group symmetry is 4/mmm as determined from data scaling statistics. Assuming one monomer of Rad53-FHA1 (molecular mass of 17 289 Da) in the asymmetric unit, the V_M (Matthews, 1968) value is 2.9 Å^3 Da^{-1}, corresponding to a crystal solvent content of 57%. Attempts to

Figure 1
Crystal of Dun1-FHA with approximate dimensions of 0.1 $\times$ 0.2 $\times$ 0.2 mm.

Table 1
X-ray diffraction data-collection statistics of Dun1-FHA and Rad53-FHA1 domains.

Values in parentheses represent the highest resolution shell.

	Dun1p FHA	Rad53p FHA1
Space group	$P6_122$ or $P6_522$	Laue group 4/mmm
Unit-cell parameters (Å)	$a = b = 127.3$,	$a = b = 61.7$,
	$c = 386.3$	$c = 104.3$
Resolution range (Å)	100–3.1 (3.21–3.10)	30.0–4.0 (4.14–4.00)
Measured reflections	1521431	12002
Unique reflections	34158 (3376)	1816 (178)
Completeness (%)	98.2 (99.9)	93.3 (94.2)
Average $I/\sigma(I)$	21.1 (2.7)	4.6 (1.9)
R_{merge}† (%)	10.8 (98.8)	33.0 (76.9)

† $R_{merge} = \sum_{hkl}[\sum_i(|I_{hkl,i} - \langle I_{hkl,i}\rangle|)]/\sum_{hkl,i}\langle I_{hkl}\rangle$, where $I_{hkl,i}$ is the intensity of an individual measurement of the reflection with Miller indices h, k and l, and $\langle I_{hkl}\rangle$ is the average intensity of that reflection calculated for $I > -3\sigma(I)$.

solve the crystal structure by molecular replacement are in progress, as are further crystallization experiments to obtain suitable crystals for cryocooled X-ray data collection and improved data quality.

Structural studies of FHA domains alone and in complex with phosphorylated target peptides will provide atomic details of the interactions that facilitate recognition and binding between these non-catalytic modules and their protein partners. Consequently, this will contribute to the understanding of the mechanism of formation of protein signalling complexes and the regulation of complex cellular signalling pathways.

References

Bell, D. W., Varley, J. M., Szydlo, T. E., Kang, D. H., Wahrer, D. C., Shannon, K. E., Lubratovich, M., Verselis, S. J., Isselbacher, K. J., Fraumeni, J. F., Birch, J. M., Li, F. P., Garber, J. E. & Haber, D. A. (1999). *Science*, **286**, 2528–2531.

Carney, J. P., Maser, R. S., Olivares, H., Davis, E. M., Le Beau, M., Yates, J. R. III, Hays, L., Morgan, W. F. & Petrini, J. H. (1998). *Cell*, **93**, 477–486.

Collaborative Computational Project, Number 4 (1994). *Acta Cryst.* D**50**, 760–763.

Durocher, D., Henckel, J., Fersht, A. R. & Jackson, S. P. (1999). *Mol. Cell*, **4**, 387–394.

Elledge, S. J. (1996). *Science*, **274**, 1664–1672.

Hammet, A., Pike, B. L., Mitchelhill, K. I., Teh, T., Kobe, B., House, C. M., Kemp, B. E. & Heierhorst, J. (2000). *FEBS Lett.* **471**, 141–146.

Hofmann, K. & Bucher, P. (1995). *Trends Biochem. Sci.* **20**, 347–349.

Jancarik, J. & Kim, S.-H. (1991). *J. Appl. Cryst.* **24**, 409–411.

Liao, H., Byeon, I. J. & Tsai, M. D. (1999). *J. Mol. Biol.* **294**, 1041–1049.

McPherson, A. (1982). *Preparation and Analysis of Protein Crystals.* New York: Wiley.

Matthews, B. W. (1968). *J. Mol. Biol.* **33**, 491–497.

Otwinowski, Z. & Minor, W. (1997). *Methods Enzymol.* **276**, 307–326.

Pawson, T. & Scott, J. D. (1997). *Science*, **278**, 2075–2080.

Rhind, N. & Russel, P. (1998). *Curr. Opin. Cell. Biol.* **10**, 749–758.

Scolnick, D. M. & Halazonetis, T. D. (2000). *Nature (London)*, **406**, 430–435.

Sun, Z., Hsiao, J., Fay, D. S. & Stern, D. F. (1998). *Science*, **281**, 272–274.

Vagin, A. A. & Teplyakov, A. (1997). *J. Appl. Cryst.* **30**, 1022–1025.